Since January 2020 Elsevier has created a COVID-19 resource centre with free information in English and Mandarin on the novel coronavirus COVID-19. The COVID-19 resource centre is hosted on Elsevier Connect, the company's public news and information website.

Pulmonary Pharmacology & Therapeutics 80 (2023) 102189

Contents lists available at ScienceDirect

Pulmonary Pharmacology & Therapeutics

journal homepage: www.elsevier.com/locate/ypupt

Establishment of multicenter COVID-19 therapeutics preclinical test system in Republic of Korea

Hyuna Noh [a,1], Suhyeon Yoon [a,1], Sung-Hee Kim [b,1], Jiseon Kim [b], Jung Seon Seo [b], Jeong Jin Kim [b], In Ho Park [b,c], Jooyeon Oh [d], Joon-Yong Bae [e], Gee Eun Lee [e], Sun-Je Woo [f], Sun-Min Seo [g], Na-Won Kim [g], Youn Woo Lee [h], Hui Jeong Jang [h], Seung-Min Hong [i], Se-Hee An [i], Kwang-Soo Lyoo [j], Minjoo Yeom [k], Hanbyeul Lee [k], Bud Jung [k], Sun-Woo Yoon [l], Jung-Ah Kang [l], Sang-Hyuk Seok [m], Yu Jin Lee [m], Seo Yeon Kim [n], Young Been Kim [n], Ji-Yeon Hwang [n], Dain On [a,o], Soo-Yeon Lim [a], Sol Pin Kim [a], Ji Yun Jang [p,q], Ho Lee [p], Kyoungmi Kim [r], Hyo-Jung Lee [s], Hong Bin Kim [t], Sun Bean Kim [u], Jun Won Park [m], Dae Gwin Jeong [l], Daesub Song [k], Kang-Seuk Choi [i], Ho-Young Lee [h], Yang-Kyu Choi [g], Jung-ah Choi [f], Manki Song [f], Man-Seong Park [e], Jun-Young Seo [b], Jeon-Soo Shin [b,c,d], Jun-Won Yun [v,**], Ki Taek Nam [b,***], Je Kyung Seong [a,o,w,*]

[a] Korea Mouse Phenotyping Center, Seoul National University, Seoul, 08826, Republic of Korea
[b] Severance Biomedical Science Institute, Brain Korea 21 PLUS Project for Medical Science, Yonsei University College of Medicine, Seoul, 03722, Republic of Korea
[c] Institute of Immunology and Immunological Diseases, Yonsei University College of Medicine, Seoul, 03722, Republic of Korea
[d] Department of Microbiology, Yonsei University College of Medicine, Seoul, 03722, Republic of Korea
[e] Department of Microbiology, Institute for Viral Diseases, Biosafety Center, Korea University College of Medicine, Seoul, 02841, Republic of Korea
[f] Science Unit, International Vaccine Institute, Seoul, 08826, Republic of Korea
[g] Department of Laboratory Animal Medicine, College of Veterinary Medicine, Konkuk University, Seoul, 05029, Republic of Korea
[h] Department of Nuclear Medicine, Seoul National University Bundang Hospital, Seongnam, 13488, Republic of Korea
[i] Laboratory of Avian Diseases, BK21 plus Program for Veterinary Science and Research Institute for Veterinary Science, College of Veterinary Medicine, Seoul National University, Seoul, 08826, Republic of Korea
[j] Korea Zoonosis Research Institute, Chonbuk National University, Iksan, 54531, Republic of Korea
[k] Department of Pharmacy, College of Pharmacy, Korea University, Sejong, 30019, Republic of Korea
[l] Bionanotechnology Research Center, Korea Research Institute of Bioscience and Biotechnology, Daejeon, 34141, Republic of Korea
[m] Division of Biomedical Convergence, College of Biomedical Science, Kangwon National University, ChunCheon, 24341, Republic of Korea
[n] Preclinical Research Center, Seoul National University Bundang Hospital, Seongnam, 13488, Republic of Korea
[o] Laboratory of Developmental Biology and Genomics, Research Institute for Veterinary Science, and BK21 PLUS Program for Creative Veterinary Science Research, College of Veterinary Medicine, Seoul National University, Seoul, 08826, Republic of Korea
[p] Graduate School of Cancer Science and Policy, National Cancer Center, Goyang, Gyeonggi, 10408, Republic of Korea
[q] College of Pharmacy, Dongguk University, Seoul, 04620, Republic of Korea
[r] Department of Biomedical Sciences and Department of Physiology, Korea University College of Medicine, Seoul, 02841, Republic of Korea
[s] Department of Periodontology, Section of Dentistry, Seoul National University Bundang Hospital, Seongnam, 13620, Republic of Korea
[t] Department of Internal Medicine, Seoul National University Bundang Hospital, Seoul National University College of Medicine, Seongnam, 13620, Republic of Korea
[u] Division of Infectious Diseases, Department of Internal Medicine, Korea University College of Medicine, Seoul, 02841, Republic of Korea
[v] Laboratory of Veterinary Toxicology, College of Veterinary Medicine and Research Institute for Veterinary Science, Seoul National University, Seoul, 08826, Republic of Korea
[w] Interdisciplinary Program for Bioinformatics, Program for Cancer Biology and BIO-MAX/N-Bio Institute, Seoul National University, Seoul, 08826, Republic of Korea

Abbreviations: ABSL3, Animal Biosafety Level 3; COVID-19, coronavirus disease 2019; SARS-CoV-2, severe acute respiratory syndrome coronavirus 2; ACE2, angiotensin-converting enzyme 2; TMPRSS2, transmembrane protease serine 2; MOAs, mechanisms of action; DMEM, Dulbecco's modified Eagle's medium; FBS, fetal bovine serum; $TCID_{50}$, tissue culture infective dose; PFU, plaque-forming units; CPE, cytopathic effect; H&E, Hematoxylin and eosin staining; LIMS, laboratory information management system; PK, pharmacokinetics; dpi, days post-infection; NHPs, nonhuman primates; CCSP, Clara cell secretory protein; SFTPB, surfactant protein B.

* Corresponding author. Korea Mouse Phenotyping Center, Seoul National University, Seoul, 08826, Republic of Korea.
** Corresponding author. Laboratory of Veterinary Toxicology, College of Veterinary Medicine, Seoul National University, Seoul, 08826, Republic of Korea.
*** Corresponding author.
E-mail addresses: jwyun@snu.ac.kr (J.-W. Yun), kitaek@yuhs.ac (K.T. Nam), snumouse@snu.ac.kr (J.K. Seong).
[1] Equal first authors.

https://doi.org/10.1016/j.pupt.2023.102189
Received 21 September 2022; Received in revised form 3 January 2023; Accepted 8 January 2023
Available online 10 January 2023

ARTICLE INFO

Keywords:
SARS-CoV-2
COVID-19
Nonclinical
hACE2 mouse
Golden Syrian hamster

ABSTRACT

Throughout the recent COVID-19 pandemic, South Korea led national efforts to develop vaccines and therapeutics for SARS-CoV-2. The project proceeded as follows: 1) evaluation system setup (including Animal Biosafety Level 3 (ABSL3) facility alliance, standardized nonclinical evaluation protocol, and laboratory information management system), 2) application (including committee review and selection), and 3) evaluation (including expert judgment and reporting). After receiving 101 applications, the selection committee reviewed pharmacokinetics, toxicity, and efficacy data and selected 32 final candidates. In the nonclinical efficacy test, we used golden Syrian hamsters and human angiotensin-converting enzyme 2 transgenic mice under a cytokeratin 18 promoter to evaluate mortality, clinical signs, body weight, viral titer, neutralizing antibody presence, and histopathology. These data indicated eight new drugs and one repositioned drug having significant efficacy for COVID-19. Three vaccine and four antiviral drugs exerted significant protective activities against SARS-CoV-2 pathogenesis. Additionally, two anti-inflammatory drugs showed therapeutic effects on lung lesions and weight loss through their mechanism of action but did not affect viral replication. Along with systematic verification of COVID-19 animal models through large-scale studies, our findings suggest that ABSL3 multicenter alliance and nonclinical evaluation protocol standardization can promote reliable efficacy testing against COVID-19, thus expediting medical product development.

1. Introduction

The etiology of the coronavirus disease 2019 (COVID-19) pandemic is a novel severe acute respiratory syndrome coronavirus 2 (SARS-CoV-2), which was originally identified in Wuhan, China, in early December 2019. Within four months, it spread across many countries, causing a major global public health concern owing to its rapid transmission [1,2]. For infection with SARS-CoV-2, an enveloped single-stranded RNA virus [3], the spike (S) protein on the surface of this virus plays a key role in host receptor recognition and binding to promote virus entry into cells [4]. In particular, it requires angiotensin-converting enzyme 2 (ACE2) for viral cell entry and transmembrane protease serine 2 (TMPRSS2) for S protein priming [4]. Once the virus enters alveolar epithelial cells in the lungs, rapid viral replication triggers an aberrant host immune response called a cytokine storm, which is characterized by the release of a series of cytokines including tumor necrosis factor-α, interleukin-1, and interleukin-6 [5,6]. These factors induce acute respiratory distress with excessive inflammation [7].

To overcome the current COVID-19 pandemic, global efforts are underway to develop appropriate diagnostic and treatment approaches as well as vaccines for SARS-CoV-2 infection. Addressing prior challenges in vaccine development (e.g., live-attenuated viruses and recombinant vector-based, protein subunits-based, or nucleic acid-based platforms) against Middle East respiratory syndrome and SARS could facilitate the development of an effective COVID-19 vaccine [8], which is critical to reach herd immunity and suppress the spread of the virus. In addition to vaccines, many pharmaceutical options for COVID-19 therapies are rapidly developing with increasingly an improving understanding of various mechanisms of action (MOAs). Because SARS-CoV-2 S protein binding with ACE2 is a well-known necessary step for viral entry, this mechanism can be a potential therapeutic target for the development of effective antiviral drugs for COVID-19 [9]. It is widely believed that neutralizing antibodies can block S protein binding to host cell receptors, such as ACE2 [10]. Additionally, an inhibitor targeting another viral entry protein, TMPRSS2, including camostat mesylate, has been shown to reduce the incidence of COVID-19 [11]. Furthermore, evidence shows that COVID-19-associated lung fibrosis is associated with unregulated immune/inflammatory mechanisms as a result of a cytokine storm [7]. For example, pirfenidone has been shown to have significant antifibrotic and anti-inflammatory properties, resulting in a possible treatment option for lung lesions involving COVID-19 [12,13].

Recently, many additional therapeutic and vaccine candidates have been applied in nonclinical trials using monkey, ferret, hamster, and human ACE2 (hACE2) transgenic mice models [14,15] demonstrated that Syrian hamsters are highly susceptible to SARS-CoV-2 infection with severe pathological lung lesions, indicating that this could be a suitable mammalian model for studying COVID-19. In addition [16], found that transgenic mice expressing hACE2, which is the main entry receptor for SARS-CoV2, showed weight loss and typical histopathology with interstitial pneumonia as well as virus replication after SARS-CoV-2 infection, demonstrating that the hACE2 mouse model could be valuable for understanding the pathogenesis of COVID-19. Throughout the COVID-19 pandemic, the South Korean government has extensively supported the research and development of effective vaccines and therapeutics against SARS-CoV-2 using national funding. In this study, we introduce a nonclinical efficacy evaluation system using the Animal Biosafety Level 3 (ABSL3) multicenter alliance system based on national support for potential vaccines and therapeutic agents to prevent or treat COVID-19. In addition, we performed comprehensive analyses of *in vivo* nonclinical efficacy data for 32 candidates from pharmaceutical companies, biotech entities, and laboratories at academic institutions.

2. Materials and methods

2.1. Cell culture and SARS-CoV-2 propagation

An African green monkey kidney cell line (Vero E6) was obtained from the American Type Culture Collection (Manassas, VA, USA) or the Korean Collection for Type Cultures (Daejeon, South Korea). Cells were cultured in Dulbecco's modified Eagle's medium (DMEM) supplemented with 5%–10% fetal bovine serum (FBS) and antibiotics in a 37 °C humidified 5% CO_2 incubator. SARS-CoV-2 (NCCP43326, BetaCoV/Korea/KCDC03/2020) was obtained from the National Culture Collection for Pathogens, Korea Disease Control and Prevention Agency (Osong, South Korea) and amplified in Vero E6 cells. SARS-CoV-2 was inoculated into Vero E6 to confirm the cytopathic effect consisting of rounding and detachment of cells, and the virus titer was measured by plaque assay. All studies on SARS-CoV-2 were conducted in ABSL3 facilities and approved by the Institutional Biosafety Committee or the Institutional Safety Committee of Yonsei University Health System (Seoul, South Korea), Seoul National University Bundang Hospital (Seongnam, South Korea), Konkuk University (Seoul, South Korea), Korea University College of Medicine (Seoul, South Korea), the International Vaccine Institute (Seoul, South Korea), and Jeonbuk National University (Iksan, South Korea).

2.2. Animal experiment

For animal experiments, specific-pathogen-free 6–14-week-old male transgenic mice expressing hACE2 under a cytokeratin 18 promoter

(K18) (Jackson Laboratories, Bar Harbor, ME, USA) and 9–14-week-old male golden Syrian hamsters (Japan SLC Inc., Shizuoka, Japan) were maintained under controlled normal atmospheric temperature (23 ± 3 °C) and relative humidity (50 ± 10%) during a 12-h light–dark cycle. The mice were fed a natural ingredient diet, Harlan 2918C (Raon Bio, Yongin, South Korea), and the hamsters were fed a normal diet of laboratory rodent chow (Cargill Agri Purina, Inc., Seongnam, South Korea) with tap water *ad libitum*. The hACE2 mice and golden Syrian hamsters were anesthetized with 2% isoflurane, followed by intranasal inoculation of SARS-CoV-2 stock virus at a dose of 10^4–10^6 50% tissue culture infective dose ($TCID_{50}$) or plaque-forming units (PFU). The animals were observed to record mortality, clinical signs, and body weight by properly trained and qualified individuals at least once daily. Humane endpoints were determined when the animals exhibited severe weight loss, signs of illness, or abnormal behavior. When animals meeting the euthanasia criteria were found other than those that died due to SARS-CoV-2 infection, euthanasia was performed immediately. On the last day of the experiment, all surviving animals were euthanized using Zoletil/Xylazine (Yonsei University College of Medicine, Seoul National University Bundang Hospital), Alfaxalone/Xylazine (Korea University College of Medicine), isoflurane (Jeonbuk National University, Konkuk University), or carbon dioxide (the International Vaccine Institute) for blood sample collection. At sacrifice, the animals were collected different tissues to screen organ weight, viral titer, and histopathological changes. During necropsy, the lungs, liver, kidneys, and spleen were weighed and fixed in 10% neutral formalin. The lungs were immediately cryopreserved in liquid nitrogen for viral replication analysis. All experimental procedures were approved by the Institutional Animal Care and Use Committee of the Department of Laboratory Animal Resources of Yonsei University College of Medicine (2020-0216), Seoul National University Bundang Hospital (BA-2008-301-071), Konkuk University (KU20142), Korea University College of Medicine (KOREA-2020-0047), the International Vaccine Institute (2020-027), and Jeonbuk National University (JBNU-2020-63).

2.3. Virus viability and quantification

For the plaque assay, Vero E6 cells were inoculated with ten-fold serial dilutions of SARS-CoV-2 samples and adsorbed at 37 °C in a 5% CO_2 incubator for 1 h. After removing the virus mixture on the cells, a mixture of DMEM containing 2% FBS and antibiotics with low melting temperature agarose was overlaid on the cells and allowed to solidify at room temperature. To stain plaques using the agarose overlay, 4% paraformaldehyde was added on top of the agarose and incubated for 1 h. The agarose plug was removed, and the fixed monolayer was stained with 0.5% crystal violet in 20% methanol. After the cells were washed with tap water, the number of plaques was counted. Viral titers were calculated as PFU/mL. For the $TCID_{50}$ test, right half lung lobes were homogenized in 1 mL DMEM using beads, and centrifugation was performed at 13,000 rpm at 4 °C for 10 min as previously described [17]. The titer was calculated using the Spearman-Karber method. For quantitative reverse transcription PCR (RT-qPCR) of viral RNA in SARS-CoV-2 samples, we used commercially available molecular diagnostics (STANDARD M nCoV Real-Time Detection kit, SD Biosensor Inc., Suwon, South Korea; Allplex 2019-nCoV Assay, Seegene, Seoul, South Korea) or the QuantiFast SYBR® Green RT-PCR kit (QIAGEN, Hilden, Germany) with the designed specific primers according to the manufacturer's recommendations. The reaction was completed by determining the dissociation curve of all amplicons generated using the ABI 7500 device (Applied Biosystems, Weiterstadt, Germany).

2.4. Live-cell viral neutralization tests (plaque/focus reduction neutralization test)

Vero E6 cells were seeded in a 96-well cell culture plate (SPL Life Science, Pocheon, South Korea) at 1.5×10^4 cells/well and cultured in a 37 °C CO_2 incubator. Vaccine-immunized mouse serum was incubated in a 56 °C constant temperature water bath for 30 min, and each serum sample was diluted with DMEM. The SARS-CoV-2 virus was reacted with serum for 0.5–1 h in an incubator at 37 °C. After washing the Vero E6 cells, 50–100 μL of serum and virus mixture reaction solution was dispensed into each well. The virus control group proceeded in the same manner as the serum reaction group by mixing the same amount of medium instead of serum. For the plaque reduction neutralization test, five days after inoculation of the serum and virus mixture, the cytopathic effect (CPE) was observed under a microscope, and CPE was 100% inhibited and the corresponding well monolayer was determined as positive when it was morphologically compared with the well of the normal cell control group. The antibody titer was the reciprocal of the maximum dilution factor that did not cause a cytopathic effect. For the focus reduction neutralization test, Vero E6 cells were fixed with 4% paraformaldehyde in PBS at 4 °C. The plates were washed and sequentially incubated with anti-SARS-CoV-2 antibody and HRP-conjugated goat anti-rabbit IgG. SARS-CoV-2-infected cell foci were visualized using TMB substrate and quantitated on an ELISPOT reader (CTL S5 Micro Analyzer, Cellular Technology Limited, Shaker Heights, OH, USA).

2.5. Histopathological changes in the liver and spleen

Animal tissues were fixed in 10% neutral buffered formalin, processed routinely, and embedded in paraffin. Hematoxylin and eosin staining (H&E) was performed on 3 μm thick serial sections from tissue paraffin blocks. The lesions were graded using a semiquantitative scale based on the percentage of tissue affected by change [18,19]: 0, absent; 1, minimal, less than 10% of tissue affected; 2, mild, more than 10% but less than 25% of tissue affected; 3, moderate, more than 25% but less than 50% of tissue affected; 4, moderately severe, more than 50% but less than 75% of tissue affected; and 5, severe, more than 75% of the affected tissue. According to previous studies on COVID-19-associated pulmonary lesions [20,21], we evaluated the presence and abundance of the following: (1) pulmonary inflammation, involving perivascular/peribronchial spaces with a moderate number of inflammatory cells encircling the regions and interstitial spaces with more than five inflammatory cells in the alveolar space; (2) pulmonary edema, involving the perivascular spaces exhibiting edematous cuffs and alveolar edematous spaces; and (3) capillary dilatation involving interstitial spaces with congested and/or dilated capillaries. To evaluate splenic lesions following SARS-CoV-2 infection [22], the scoring for apoptosis/necrosis and atrophy within the white pulp of mice was determined based on the extent of the affected area. Histopathological scores were independently determined by two experienced veterinary pathologists (K.T.N. and J.W.P.).

2.6. Statistical analysis

The results are expressed as the mean ± SE. Data were analyzed by Student's t-test or one-way analysis of variance using SPSS software version 19 (SPSS Inc., Chicago, IL, USA). The level of significance was set at $p < 0.05$, or $p < 0.01$.

3. Results

3.1. Establishment of multicenter COVID-19 efficacy evaluation system

To develop vaccines and therapeutics for SARS-CoV-2 prevention and treatment, we first established a multicenter ABSL3 facility alliance consisting of six ABSL3 facilities in South Korea for rapid preclinical animal studies of large numbers of substances (Fig. 1). A standardized protocol for nonclinical evaluation was also developed for reliable nonclinical efficacy evaluation by multicenter ABSL3 facilities. First, animal disease models were established, including mice expressing

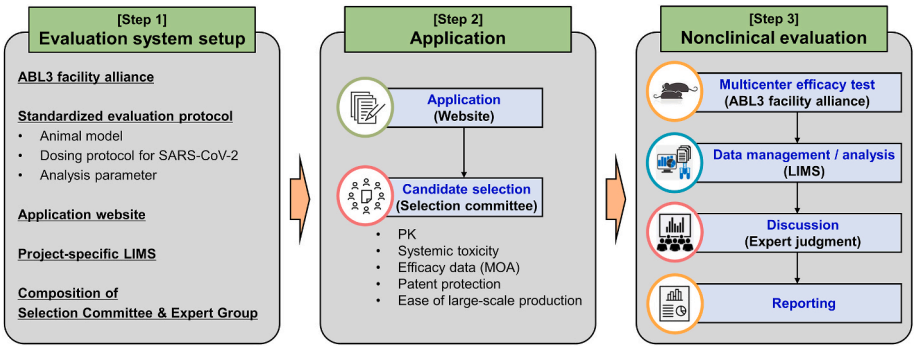

Fig. 1. Establishment of nonclinical efficacy evaluation system with a multicenter ABSL3 facility alliance for SARS-CoV-2 vaccine and therapeutic development.

hACE2 under the K18 epithelial promoter and hamster model. Second, for the nonclinical efficacy test, we established a SARS-CoV-2 infection protocol and experimental analysis parameters such as mortality, clinical signs, body weight, viral titer, neutralizing antibody, and histopathology resembling the condition seen in human COVID-19 pathogenesis. Appropriate sacrifice time points that can most significantly analyze the above markers, including peak viral load or marked histopathological pulmonary findings, were selected based on the results of preliminary experiments. In addition, we developed a COVID-19-specific laboratory information management system (LIMS) to store and analyze efficacy nonclinical evaluation data in addition to application websites for COVID-19 therapeutic and vaccine candidates. Because the LIMS can be used for data storage, processing, analysis, and management in an associated environment that produces a large quantity of information, it can also play an important role in the comprehensive monitoring of multicenter laboratory large-scale data from COVID-19 nonclinical efficacy-related studies. To objectively select nonclinical test candidates from pharmaceutical companies, biotech entities, and academic laboratories during the COVID-19 pandemic, we formed a selection committee tasked with reviewing submitted documents including pharmacokinetics (PK), systemic toxicity, MOA-related preliminary efficacy data, patent-holding, and ease of large-scale production. Additionally, we managed a group discussion with experts from different fields, such as immunology, pathology, mouse phenotyping, and toxicology, to determine effective substances by analyzing data from nonclinical efficacy tests.

3.2. Candidate selection for a COVID-19 nonclinical efficacy study

We created an application website (covid19.animalmodel.kr) where various substance information and preliminary data can be entered for easy application in a COVID-19 nonclinical efficacy study. A total of 101 candidates for a nonclinical test were obtained through this established website over a six-month period. As shown in Fig. 2A, 75 candidates (74.3%) selected hACE2 transgenic mice for animal models, whereas 26 (25.7%) used the hamster model. Applications included 74 (73.3%) new drug candidates and 27 (26.7%) repositioned pre-existing drugs (Fig. 2B). Of 101 applications, 80 (79.2%) were potential therapeutics and 21 (20.8%) were vaccine candidates (Fig. 2C). After the preliminary in-depth review of submitted documents, the selection committee proceeded with second evaluation of the applicants' presentations and selected 32 final supporting candidates for the nonclinical *in vivo* efficacy study (24 (75.0%) using the hACE2 transgenic mice model and 8 (25.0%) using the hamster model; 20 (62.5%) new drug candidates and 12 (37.5%) repositioned pre-existing drugs; 26 (81.3%) potential therapeutics and 6 (18.8%) vaccine candidates).

3.3. Development of a standardized protocol for COVID-19 nonclinical efficacy study using animal models

As shown in Fig. 3A, beginning at 1 d post-infection (dpi), intranasal inoculation with SARS-CoV-2 in K18-hACE2 mice resulted in marked weight loss for up to 7 dpi. And, the hACE2 transgenic mouse model displayed high mortality from 5 dpi in the SARS-CoV-2 infection group (Fig. 3B). We also observed clinical signs with decreased activity and response to external stimuli in the SARS-CoV-2-infected hACE2 mice (data not shown). Because viral replication reached a peak at 2 dpi in the lung homogenates of the K18-hACE2 mice, the level of infectious SARS-CoV-2 declined in a time-dependent manner, although it was still detected at 7 dpi (Fig. 3C). Microscopically, H&E-stained lung sections from SARS-CoV-2-infected hACE2 mice displayed an inflammatory process, including inflammatory cell infiltration, edema, and capillary dilatation, at 2 dpi (Fig. 3D). In addition, white pulp atrophy was evident in the spleens of infected hACE2 mice. These pathological lesions in the lung and spleen worsen over time upon infection with SARS-CoV-2 up to 7 dpi.

Body weights of SARS-CoV-2-infected Syrian hamsters were 8.60% (at 3 dpi) and 12.09% (at 7 dpi) lower than to the respective control groups (Fig. 3A). However, body weight reductions of SARS-CoV-2-infected hamsters were relatively smaller than those of infected hACE2 mice. And, Syrian hamsters showed no lethal phenotype following viral infection (Fig. 3B). Infected hamsters did not exhibit any measurable clinical signs during the entire experimental period (data not shown). Levels of infectious virus in the lungs of Syrian hamsters

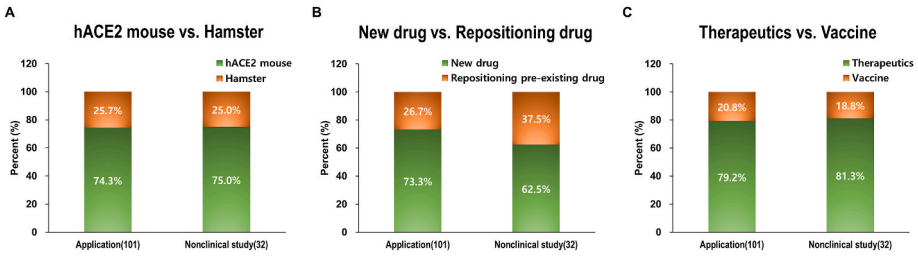

Fig. 2. Number of substances applied and tested for COVID-19 nonclinical efficacy study. Classification of 101 applications and 32 test substances according to animal models (hACE2 mice vs. hamsters) (A), development type (new development vs. repositioning) (B), and drug type (therapeutics vs. vaccines) (C). The value in parentheses represents the number of substances.

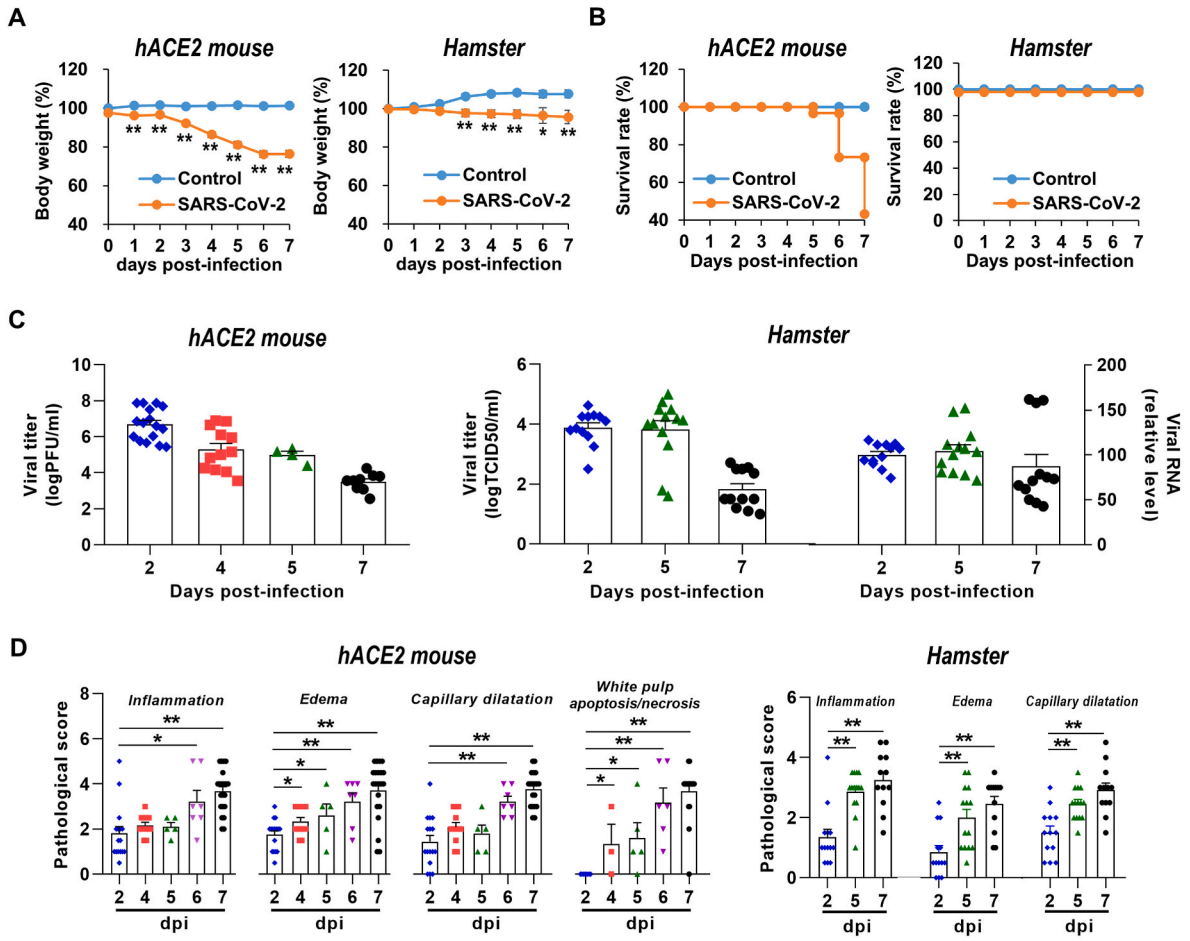

Fig. 3. Effects of SARS-CoV-2 infection in hACE2 transgenic mice and Syrian hamsters. Animals were intranasally inoculated with SARS-CoV-2 at a dosage of 10^5–10^6 $TCID_{50}$ (or PFU) and sacrificed 2 to 7 dpi. (A) Body weight changes in hACE2 mice (n = 25 for control group; n = 70 for SARS-CoV-2 group) and Syrian hamsters (n = 30 for control group; n = 30 for SARS-CoV-2 group) after viral infection. (B) Survival rate of hACE2 mice (n = 23 for control group; n = 30 for SARS-CoV-2 group) and Syrian hamsters (n = 30 for control group; n = 30 for SARS-CoV-2 group) infected with SARS-CoV-2. (C) Virus replication in lungs of infected hACE2 mice (n = 16 for 2 dpi; n = 12 for 4 dpi; n = 4 for 5 dpi; n = 9 for 7 dpi) and virus replication/RNA in lungs of Syrian hamsters (n = 12 for 2 dpi; n = 12 for 5 dpi; n = 13 for 7 dpi). (D) Pathological severity scores in lungs (n = 16 for 2 dpi; n = 12 for 4 dpi; n = 5 for 5 dpi; n = 7 for 6 dpi; n = 19–21 for 7 dpi) and spleens (n = 8 for 2 dpi; n = 3 for 4 dpi; n = 5 for 5 dpi; n = 6 for 6 dpi; n = 18 for 7 dpi) of infected hACE2 mice and lungs (n = 13 for 2 dpi; n = 14 for 5 dpi; n = 12 for 7 dpi) of Syrian hamsters. Data are expressed as mean ± SE (*$p < 0.05$, **$p < 0.01$).

showed trends similar to those observed in the hACE2 mouse model, whereas high levels of viral RNA were maintained at 2, 5, and 7 dpi (Fig. 3C). Hamsters infected with SARS-CoV-2 developed varying degrees of lung injury. Histopathological examination detected an increase in focal inflammatory cells in the interstitium and alveolar cavity of the lungs at 2 dpi. At 7 dpi, there was an increase in inflammatory cell infiltration, edema, and capillary dilatation in the lungs (Fig. 3D).

3.4. *Comprehensive analysis of nonclinical efficacy studies for therapeutic and vaccine candidates against SARS-CoV-2 infection*

Table 1 summarizes the information on 32 therapeutic and vaccine candidates for COVID-19. To identify their inhibitory effects on SARS-CoV-2-related lesions in the nonclinical efficacy testing using animal disease models, we intranasally inoculated SARS-CoV-2 at a dosage of 10^4–10^6 $TCID_{50}$ (or PFU) to K18-hACE2 transgenic mice or hamsters in the presence or absence of therapeutics/vaccine candidates and analyzed various parameters involved in the infection following necropsy on 2 to 14 dpi (Fig. 4). For nonclinical efficacy studies for each substance, we consulted the application agency to determine the optimal animal model, SARS-CoV-2 infection conditions, administration schedule (i.e., dose, route, timing, and duration), and necropsy schedule.

Upon extensive discussion with experts regarding comprehensive data analysis, including of mortality, clinical signs, body weight, viral titer, neutralizing antibody, and histopathology data at the indicated time points stored in the COVID-19-specific LIMS, we concluded that 9 of the 32 candidates showed MOA-related partial or high efficiency in the prevention or treatment of COVID-19 lesions in animal disease models through nonclinical tests (Table 2). As indicated in Fig. 5, eight effective substances (88.9%) were tested using the hACE2 transgenic mouse model, while one (11.1%) was tested using the hamster model. These nine effective substances included eight new drugs (88.9%) and one repositioned pre-existing drug (11.1%). Of the nine candidates showing significant efficacy, three (33.3%) were vaccines and six (66.7%) were therapeutics, including four anti-viral agents and two anti-inflammatory agents. Among them, substance #6, a new vaccine candidate, has shown the ability to produce neutralizing antibodies and block all COVID-19-related lesions, including histopathological lung and spleen lesions, body weight loss, and viral replication in SARS-CoV-2-treated hACE2 mice. In contrast, substance #16, a new vaccine candidate, enhanced neutralizing antibody production and exhibited inhibitory activities against SARS-CoV-2-related body weight loss, mortality, increased lung viral titer, and histopathological lung (pulmonary edema) and spleen (white pulp atrophy and necrosis) lesions in nonclinical testing using the hACE2 mouse model, although they did not

Table 1
Information of nonclinical efficacy evaluation for 32 therapeutic and vaccine candidates targeting COVID-19.

No	Category		Test substance				Animal model		Virus (NCCP 43326)		Necropsy schedule	ABL3 institute[c]
			MOA[a]	LIMS No.	Dose schedule	Route			Dose	Route		
1	Treatment	Repositioning	Anti-viral	KP1	once (1 dpi)	IM	Hamster	M48 (13 w)[b]	$10^{5.5}$	IN	2,5,7 dpi	KP
2	Treatment	New development	Anti-viral	KP2	bid (1–3 dpi)	IP	Hamster	M48 (13 w)	$10^{5.5}$	IN	2,5,7 dpi	KP
3	Treatment	New development	Anti-inflammation	KM2	bid (0 dpi), qd (1–7 dpi)	IP	hACE2 mouse	M30 (13 w)	10^{6}	IN	2,4,7–14 dpi	KM
4	Treatment	Repositioning	Anti-viral	KM1	once (0 dpi)	IP	hACE2 mouse	M38 (10 w)	10^{6}	IN	3,5,5–14 dpi	KM
5	Treatment	New development	Anti-viral/Anti-inflammation	IV3	qd (1–5 dpi)	IP	hACE2 mouse	M40 (14 w)	10^{5}	IN	2,7, 7–14 dpi	IVI
6	Vaccine	New development	Subunit	SB1	twice (2w interval)	IM	hACE2 mouse	M86 (10 w)	10^{6}	IN	2,5,7–14 dpc	SNUBH
7	Treatment	New development	Anti-viral	YM1	once (0 dpi)	IP	hACE2 mouse	M40 (9 w)	10^{6}	IN	3,5,7,10 dpi	YM
8	Treatment	Repositioning	Anti-viral/Anti-inflammation	YM6	qd (0–7 dpi)	PO	hACE2 mouse	M40 (13 w)	10^{6}	IN	2,7, 7–14 dpi	YM
9	Treatment	Repositioning	Anti-viral	IV5	qd (0 dpi), bid (1–2 dpi)	IP	Hamster	M40 (9 w)	10^{5}	IN	3,7 dpi	IVI
10	Treatment	Repositioning	Anti-viral	KP5	qd (0–4 dpi)	PO	Hamster	M36 (14 w)	$10^{5.5}$	IN	2, 5 dpi	KP
11	Treatment	Repositioning	Anti-viral	KP6	qd (0–4 dpi)	PO/IP	hACE2 mouse	M36 (14 w)	$10^{5.5}$	IN	2, 5 dpi	KP
12	Treatment	Repositioning	Anti-viral	KV1	qd (0–6 dpi)	IP	hACE2 mouse	M50 (11 w)	5×10^{5}	IN	2,7, 7–14 dpi	KV
13	Treatment	Repositioning	Anti-viral	KM3	bid (−1, 1 dpi), tid (0 dpi)	PO	Hamster	M40 (11 w)	10^{6}	IN	1,3 dpi	KM
14	Vaccine	New development	Subunit	KP3	twice (2w interval)	IM	Hamster	M36 (14 w)	$10^{5.5}$	IN	2,5,7 dpc	KP
15	Treatment	New development	Anti-viral	KP4	qd (0–4 dpi)	IP	Hamster	M36 (14 w)	$10^{5.5}$	IN	2,5,7 dpi	KP
16	Vaccine	New development	Viral vector	IV4	twice (2w interval)	IM	hACE2 mouse	M44 (11 w)	5×10^{5}	IN	2,4,7–14 dpc	IVI
17	Treatment	New development	Anti-viral/Anti-inflammation	SB4	qd (0–3 dpi)	IP	Hamster	M36 (9 w)	10^{5}	IN	2,5,7 dpi	SNUBH
18	Vaccine	New development	DNA	SB2	twice (2w interval)	IM	hACE2 mouse	M39 (12 w)	10^{5}	IN	1,3,7 dpc	SNUBH
19	Treatment	New development	Anti-viral	YM8	once (0 dpi)	IP	hACE2 mouse	M48 (11 w)	10^{6}	IN	2,4,7–14 dpi	YM
20	Treatment	Repositioning	Anti-viral	KV2	bid (0–2 dpi)	IN	hACE2 mouse	M45 (11 w)	5×10^{5}	IN	2,4,7–14 dpi	KV
21	Vaccine	New development	Synthetic peptide	SB3	three times (1w interval)	IM	hACE2 mouse	M37 (8 w)	10^{4}	IN	2,4,7 dpc	SNUBH
22	Treatment	Repositioning	Anti-viral	YM9	bid (0–2 dpi), qd (3-6dpi)	PO	hACE2 mouse	M41 (9 w)	10^{5}	IN	2,4,7–14 dpi	YM
23	Treatment	New development	Anti-inflammation	KV3	qd (1–3 dpi)	IP	hACE2 mouse	M39 (9 w)	5×10^{5}	IN	4,7,7–14 dpi	KV
24	Treatment	New development	Anti-viral	SB6	qd (0–4 dpi)	IP	hACE2 mouse	M41 (9 w)	10^{5}	IN	2,4,7 dpi	SNUBH
25	Treatment	New development	Anti-viral/Anti-inflammation	KV4	once (0 dpi)	IP	hACE2 mouse	M34 (9 w)	5×10^{5}	IN	2,4,7–14 dpi	KV
26	Treatment	New development	Anti-inflammation	YM10	bid (0–1 dpi), qd (2-6dpi)	PO	hACE2 mouse	M45 (9 w)	10^{5}	IN	2,5,7–14 dpi	YM
27	Treatment	Repositioning	Anti-viral	KV5	qd (0–4 dpi)	PO	hACE2 mouse	M43 (10 w)	10^{4}	IN	2,4,7–14 dpi	KV
28	Treatment	Repositioning	Anti-viral	KV6	qd (0–4 dpi)	PO	hACE2 mouse	M43 (9 w)	10^{4}	IN	2,4,7–14 dpi	KV
29	Vaccine	New development	Subunit	IV6	twice (2w interval)	IM	hACE2 mouse	M42 (6 w)	5×10^{5}	IN	2,4,7 dpc	IVI
30	Treatment	New development	Anti-viral	KM4	qd (−1, 1 dpi)	IN	hACE2 mouse	M37 (9 w)	10^{4}	IN	2,4,7–14 dpi	KM
31	Treatment	New development	Anti-inflammation	YM18	bid (0–6 dpi)	PO	hACE2 mouse	M39 (9 w)	10^{5}	IN	4, 7 dpi	YM
32	Treatment	New development	Anti-inflammation	SB12	once (0 dpi)	IV	hACE2 mouse	M21 (10 w)	10^{4}	IN	7dpi	SNUBH

[a] Mechanism of action.
[b] Sex, number, and age of animals tested.
[c] KP, Korea University College of Pharmacy; KM, Korea University College of Medicine; IVI, International Vaccine Institute; SNUBH, Seoul National University Bundang Hospital; YM, Yonsei University College of Medicine; KV, Konkuk University College of Veterinary Medicine.

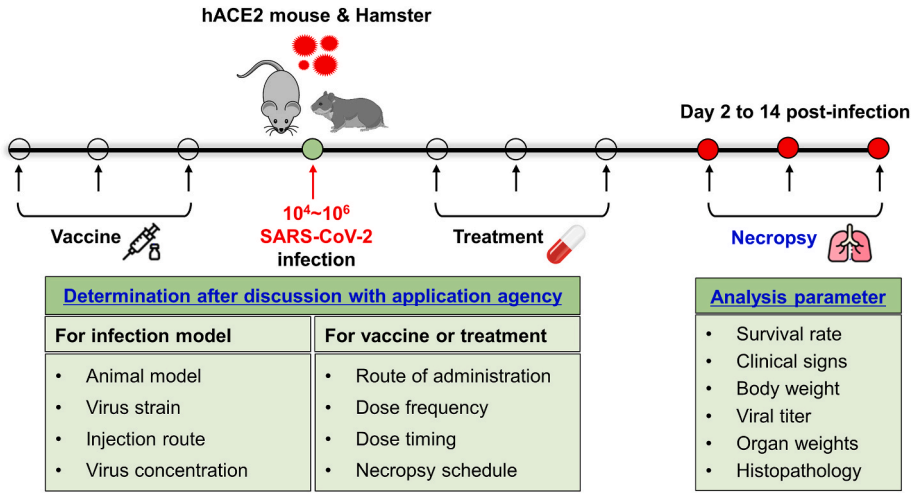

Fig. 4. Experimental scheme of COVID-19 nonclinical efficacy study using animal disease models associated with SARS-CoV-2 infection.

significantly prevent lung inflammation. Another new vaccine candidate, substance #29, also exerted neutralizing antibody production and had protective effects on body weight loss, mortality, high viral titer, and lung (pulmonary edema and capillary dilatation) and spleen (white pulp atrophy and necrosis) lesions observed in the infected hACE2 mice, although there was no significant difference in lung inflammation between the virus control and vaccine treatment groups.

Substance #7, which exhibits antiviral activities against COVID-19, has been shown to reduce body weight loss, mortality, viral replication, and lung lesions in SARS-CoV-2-treated hACE2 mice. Antiviral drug candidate #12 effectively managed body weight loss, viral replication, and histopathological pulmonary lesions, including inflammation and edema, although it did not significantly improve the survival of the infected hACE2 mice. Treatment with the new antiviral drug substance #19 resulted in a significant reduction in body weight loss, mortality, high viral replication, and histopathological lung and spleen lesions of white pulp necrosis in the infected hACE2 mouse model. Substance #15 was tested using a hamster model for SARS-CoV-2 infection. As a new antiviral drug candidate, we found that substance #15 exhibited inhibitory effects on COVID-19-related viral replication and lung lesions observed in infected hamsters.

Based on the preliminary data, the potential MOAs of substances #26 and #31, new drug candidates, are believed to exhibit anti-inflammatory action. In the current study, we found that the treatment of substance #26 in infected hACE2 mice led to reductions in body weight loss and lung injury induced by SARS-CoV-2. Similarly, substance #31 also showed anti-inflammatory effects in the lungs of SARS-CoV-2 infected hACE2 mice, along with reductions in body weight loss.

Some substances did not provide clear evidence of efficacy but demonstrated potential for further evaluation in a later study with a modified protocol of infection model and treatment conditions. Although antiviral drug substances #9 and #24, which were tested using SARS-CoV-2-infected hamsters and hACE2 mice, respectively, significantly inhibited body weight loss and mortality, they did not alleviate viral replication and COVID-19 lung injury associated with their MOA. Synthetic peptide vaccine #21 increased the survival rate and reduced lung lesions in infected hACE2 mice whereas it had no significant effect on weight loss and viral replication involved in SARS-CoV-2 infection. A new subunit vaccine candidate #14 could not protect against COVID-19-related lesions in infected hamsters. However, it upregulated neutralizing antibody production, suggesting a further study with modification of the timing and frequency of booster immunizations. The remaining substances did not yield sufficient scientific markers indicating their potential in clinical trials; in particular, antiviral drug candidate #27 aggravated the weight loss and mortality rate in SARS-CoV-2-treated hACE2 mice, possibly owing to the toxicity of the substance.

4. Discussion

As important foundations for drug discovery, nonclinical studies are necessary to predict a drug's success in clinical testing at the stage of COVID-19 therapeutic and vaccine development. Of 101 candidates, 32 substances were finally selected from pharmaceutical companies, biotech entities, and academic laboratories that applied over a six-month period with significant interest in the research project during the current COVID-19 pandemic. For the final selection of candidate substances, the selection committee analyzed existing PK and toxicity findings that could be critical factors in determining the appropriate concentration *in vivo* in the planning and execution of nonclinical efficacy tests. In addition, preliminary efficacy data regarding antiviral and anti-inflammatory activities and neutralizing antibody production associated with their MOA were also reviewed by the selection committee. From this point of view, repurposing pre-existing medications with known dosage used, safety, and PK characteristics can be the fastest way to identify therapeutic solutions during the time-critical COVID-19 pandemic because the development of new drugs requires a long, complex, and expensive process [22–24]. In fact, due to the advantages of repurposing medications, the final selection rate of repurposing drug candidates for the nonclinical *in vivo* efficacy study slightly increased from the application rate of 26.7%–37.5%. However, most repositioned drugs so far have been the result of serendipitous discoveries rather than well-thought strategies despite a promising strategy during the COVID-19 pandemic, and it usually needs to demonstrate the MOA of the drug on diseases [25]. Indeed, it is noteworthy that only one repurposing drug candidate was included among the nine effective substances.

BSL-3 animal facilities are required for nonclinical efficacy trials of therapeutics and vaccine candidates for COVID-19. However, there are a limited number of BSL-3 animal facilities in South Korea owing to the high costs of building and operating such facilities. Thus, we established a multicenter ABSL3 facility alliance consisting of six ABSL3 facilities in South Korea for rapid and large-scale efficacy evaluation during the global pandemic of COVID-19. More importantly, for objective relative evaluation, there is an urgent need for standardization of nonclinical evaluation protocols that enhance the reliability of nonclinical trials conducted at various institutions. Therefore, the selection of an animal model is one of the most important factors. Models of SARS-CoV-2 infection include monkeys, cats, ferrets, hamsters, and hACE2 transgenic mice that reproduce the viral infection and clinical pathology

Table 2
Summary of nonclinical efficacy data on 32 therapeutic and vaccine candidates for COVID-19.

No	MOA[a]	Animal model	Neutralizing antibody	Body weight	Survival rate	Virus titer		Lung			Spleen	Efficacy evaluation[d]
						Replication	Viral RNA	Inflammation	Edema	Capillary dilatation		
1	Anti-viral	Hamster	NA[b]	–	NL[c]	–	–	–	–	–	NA	–
2	Anti-viral	Hamster	NA	–	NL	–	–	–	–	–	NA	–
3	Anti-inflammation	hACE2 mouse	NA	–	NL	–	NA	–	–	–	–	–
4	Anti-viral	hACE2 mouse	NA	–	–	–	NA	–	–	–	NA	–
5	Anti-viral/Anti-inflammation	hACE2 mouse	NA	–	–	–	NA	–	–	–	–	–
6	Subunit vaccine	hACE2 mouse	+	+	NL	+	NA	+	+	+	+	+++
7	Anti-viral	hACE2 mouse	NA	+	+	+	NA	+	+	+	+	+++
8	Anti-viral/Anti-inflammation	hACE2 mouse	NA	–	–	–	NA	–	–	–	–	–
9	Anti-viral	Hamster	NA	+	+	–	NA	–	–	–	NA	+
10	Anti-viral	Hamster	NA	NL	NL	–	–	–	–	–	NA	–
11	Anti-viral	hACE2 mouse	NA	–	NL	–	–	–	–	–	NA	–
12	Anti-viral	hACE2 mouse	NA	+	–	NA	+	+	+	NA	+	+++
13	Anti-viral	Hamster	NA	–	NL	–	NA	–	–	–	NA	–
14	Subunit vaccine	Hamster	+	NL	–	–	–	–	–	–	NA	–
15	Anti-viral	Hamster	NA	–	NL	+	+	+	+	+	NA	+++
16	Viral vector vaccine	hACE2 mouse	+	+	+	+	NA	–	+	–	+	+++
17	Anti-viral/Anti-inflammation	Hamster	NA	–	NL	–	–	–	–	–	NA	–
18	DNA vaccine	hACE2 mouse	–	–	–	–	–	–	–	–	–	–
19	Anti-viral	hACE2 mouse	NA	+	+	+	NA	+	+	+	+	+++
20	Anti-viral	hACE2 mouse	NA	–	–	NA	+	–	–	NA	–	–
21	Synthetic peptide vaccine	hACE2 mouse	NA	–	+	–	–	+	+	+	–	+
22	Anti-viral	hACE2 mouse	NA	–	–	–	NA	–	+	+	–	–
23	Anti-inflammation	hACE2 mouse	NA	–	–	NA	–	–	–	NA	–	–
24	Anti-viral	hACE2 mouse	NA	+	+	–	–	–	–	–	–	+
25	Anti-viral/Anti-inflammation	hACE2 mouse	NA	–	–	NA	–	–	–	NA	+	–
26	Anti-inflammation	hACE2 mouse	NA	+	–	–	NA	+	+	+	–	++
27	Anti-viral	hACE2 mouse	NA	–	–	NA	–	+	–	NA	–	–
28	Anti-viral	hACE2 mouse	NA	–	–	NA	–	–	–	NA	–	–
29	Subunit vaccine	hACE2 mouse	+	+	+	+	NA	–	+	+	+	+++
30	Anti-viral	hACE2 mouse	NA	–	–	–	NA	–	–	–	–	–
31	Anti-inflammation	hACE2 mouse	NA	+	–	–	NA	+	+	+	–	++
32	Anti-inflammation	hACE2 mouse	NA	–	–	–	–	–	–	–	–	–

[a] Mechanism of action.
[b] Not analyzed.
[c] No lesion in virus-treated group.
[d] +, Partial efficacy; ++, Partial efficacy with effectiveness in MOA-related parameter; +++ High-potential efficacy.

observed in humans [14]. Among them, the transgenic mice expressing hACE2 under the K18 epithelial promoter [26] showed replication of the virus in the lungs, resulting in local and systemic lesions, such as pulmonary pathology, weight loss, and death within days post-infection [27,28], indicating that they can be a useful model for assessing protective or therapeutic interventions for severe COVID-19, although it is necessary to adjust the virus concentration to examine the long-term efficacy of drugs against mild COVID-19. In addition, SARS-CoV-2 infection in golden Syrian hamsters that have high similarity to hACE2 showed high lung viral replication and pathology in the respiratory tract but not weight loss [27]. Moreover, the use of ferrets among well-known animal models for SARS-CoV-2 infection has been limited because of the low availability of animals and the low number of vendors [29]. Despite their phylogenetic similarity, nonhuman primates (NHPs) may not be suitable for large-scale experiments because of high study costs, ethical considerations, and unique facility and personnel

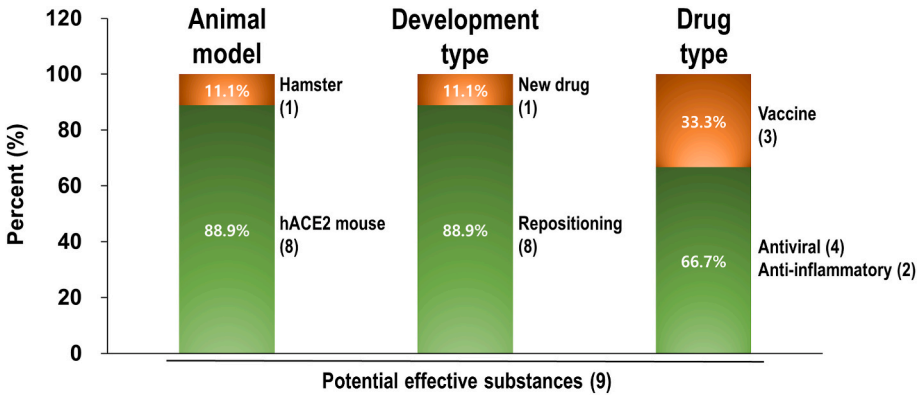

Fig. 5. Effective substances obtained from COVID-19 nonclinical efficacy study. Classification of 9 potential effective substances according to animal models (hACE2 mice vs. hamsters), development type (new development vs. repositioning), and drug type (therapeutics vs. vaccines). The value in parentheses represents the number of substances.

requirements [30], suggesting that it can be a good animal model for further confirmation studies. Thus, we selected and used K18-hACE2 transgenic mice and hamsters as animal models that mimic the biology of human SARS-CoV-2 infection for rapid preclinical efficacy studies of large numbers of substances in this study. More importantly, many applications (75 of the 101) selected a mouse model rather than hamsters for a nonclinical *in vivo* efficacy study. Of note, among the nine effective substances from COVID-19 nonclinical testing, the efficacy of only one substance was identified using the hamster model. In our recent study on comparison of the pathogenesis of SARS-CoV-2 infection between K18-hACE2 mice and Syrian hamsters, we also observed that SARS-CoV-2-infected hamsters showed significant but slight weight loss following virus infection, in comparison to infected hACE2 mice [31] in consistent with our results in the present study. More importantly, decreased body weights of infected hamsters were almost completely recovered from 6 to 8 dpi to 10 dpi [31]. Therefore, this relatively low applicability of the hamster model for COVID-19 might be due to a significant drawback associated with spontaneous recovery of lung pathology in the later stages of infection [32]. This led us to use the hamster model to identify the short-term efficacy of drugs on mild COVID-19 lesions associated with SARS-CoV-2 infection.

Potential therapeutic strategies against SARS-CoV-2 virus replication in the lungs and its inflammatory and immune complications include antiviral and anti-inflammatory therapies [33]. Although some drugs such as antiviral remdesivir [34,35] and anti-inflammatory dexamethasone [36] have been shown to be beneficial to certain groups of patients with COVID-19, their efficacies can be rather limited [33,37], leading to continued development efforts to discover effective vaccination or therapeutics including direct-acting antivirals or immunomodulatory substances. Therefore, it is also very important to establish detailed MOA-specific protocols for the nonclinical evaluation of substances with these two major MOAs. Among the analysis parameters, including mortality, clinical signs, body weight, viral titer, and histopathology, which are related to the SARS-CoV-2 pathogenesis observed in humans, the peak of viral replication was observed in lung homogenates of K18-hACE2 mice at 2 dpi in the present study. Subsequently, the infectious SARS-CoV-2 continued to decrease. Histopathological lesions observed in mouse lungs within 7 days after SARS-CoV-2 infection are characterized by acute inflammatory responses. In the early stage of virus infection, capillary dilatation (leading to an increase in blood flow) and perivascular edema (due to increased permeability of the microvasculature) are predominant. In the late stage of virus infection, emigration and infiltration of many inflammatory cells are additionally observed with capillary dilatation and edema. Our results indicated that at 2 dpi, K18-hACE2 mice showed lung lesions, including inflammatory cell infiltration, edema, and capillary dilatation. At 7 dpi, the infected mice had more severe lung inflammatory damage, even if the infectious virus was reduced. Consistent with a previous study [38], golden Syrian hamsters with SARS-CoV-2 infection showed peak viral load in the lungs at 2 to 5 dpi, followed by rapid infectious virus clearance by 7 dpi. In contrast, histopathological examination indicated that the infected hamsters had a high severity score of lung abnormalities at 7 dpi. Therefore, depending on the MOA of test substances, the optimal necropsy date should be well planned, such as early time point (2–5 dpi) for viral replication and late point (7–14 dpi) for multiorgan histopathological examination.

Of the 32 substances assessed in the current study, 9 substances showed significant efficacy, excluding 23 substances that showed a lack of efficacy or the presence of toxic properties. Nine effective substances included three vaccine candidates and six therapeutics, including four antiviral agents and two anti-inflammatory agents. First, in the case of three vaccine candidates, a marked decrease in virus titer was observed along with the recovery of body weight loss and mortality. However, their protective activity against COVID-19-associated histopathological pulmonary lesions characterized by inflammation, edema, and capillary dilatation [20,21] were found to differ depending on the substance. Although substances #16 and #29 reduced edema and capillary dilatation observed in the early stage of virus infection, the infiltration of immune cells was maintained, possibly due to the remaining infectious virus or damaged tissues associated with insufficient effectiveness of the vaccine against SARS-CoV-2 infection. Substance #6 significantly reduced inflammatory cell infiltration, edema, and capillary dilatation, indicating its protective efficacy against viral replication in the lung. This led us to suggest that changes in the above-mentioned histopathological parameters of the lungs must be verified for reliable evaluation using different animal models with SARS-CoV-2 infection, although the protective ability of a vaccine against COVID-19-related mortality is the most important efficacy endpoint [39]. Moreover, four antiviral drug candidates showed marked efficacy in terms of body weight loss, mortality, viral replication, and multiorgan histopathological lesions in both hACE2 mouse and hamster models, demonstrating that they efficiently reduced the viral load in the lung tissue of SARS-CoV-2-infected animals and subsequently inhibited the pathological lung lesions. In addition, two anti-inflammatory drug candidates showed therapeutic effects on lung lesions and weight loss by SARS-CoV-2 exposure, whereas they were not effective in interfering with virus production in the lung and subsequently were not associated with significant protection in spleen lesions and mortality. These results indicate that it is important to evaluate the MOA-related essential analysis parameters, including viral titers for antiviral drugs and histopathological pulmonary lesions, for anti-inflammatory drug candidates.

In summary, in this recent COVID-19 pandemic situation, we established a nonclinical efficacy evaluation system for rapid and reliable assessments with a national research project in South Korea with a

multicenter ABSL3 facility alliance and established standardized nonclinical evaluation protocol including animal models, protocols, analysis parameters, an application website, a selection committee, and COVID-19-specific LIMS. After reviewing 101 applications and testing 32 substances, we finally identified nine effective vaccines or therapeutic candidates using K18-hACE2 mice and hamsters. Along with major research achievements, our study will be meaningful to systematically verify the practical applicability of representative animal models of COVID-19 through large-scale nonclinical studies, indicating that this standardized nonclinical evaluation protocol with animal models can be optimal for identifying active substances with promising clinical potential. Based on the current results of this first screening round, various additional nonclinical animal models may be needed to derive more reliable results in clinical trials. First, for substances showing efficacy, it is necessary to study the properties against different SARS-CoV-2 variants and the detailed mechanism involved in each MOA, including antivirals, anti-inflammatory drugs, monoclonal antibodies, and immune modulators [40]. Also, they can be tested using NHPs to further improve the reliability of nonclinical data for human clinical trials. Second, for substances that did not show significant efficacy in MOA-related analysis parameters, a modified protocol for administration conditions and necropsy (i.e., route of administration, formulation, dose frequency, dose timing, and optimal necropsy schedule according to MOA), a larger sample size for adequate statistical power, or additional *in vivo* tests using other animal models may be suggested. In addition to K18-hACE2 mice that cause systemic multiorgan lesions and substantial lethal infection, which might be associated with neuroinvasion of SARS-CoV-2 affecting CNS [27] and multifocal perivascular cuffing in the brain [31], other hACE2 transgenic mouse strains using various promoters, including Clara cell secretory protein (CCSP), specifically expressed in the conducting airway epithelium of the lung [41,42], and surfactant protein B (SFTPB), which is a major component of pulmonary surfactant secreted by both alveolar type II and club lung epithelial cells [43], can be used to study lung-specific mild pathogenesis and long-term effects of vaccines and therapeutics. In addition to virus inoculation through respiratory droplets, it is also useful to establish appropriate animal models infected in a clinically similar manner such as aerosol virus exposure or direct contact between SARS-CoV-2 inoculated and naïve animals referring to the results of previous findings [16,38]. Taken together, we believe that the established nonclinical efficacy evaluation system will be of great help to the drug development process for Disease X as well as the ongoing COVID-19 pandemic.

Author statement

Conceptualization, Hyuna Noh, Suhyeon Yoon, Sung-Hee Kim, Jun-Won Yun, Ki Taek Nam, and Je Kyung Seong.

Formal analysis, Hyuna Noh, Suhyeon Yoon, Sung-Hee Kim, Ho Lee, Kyoungmi Kim, Hyo-Jung Lee, Hong Bin Kim, Sun Bean Kim, Jun Won Park, Dae Gwin Jeong, Daesub Song, Kang-Seuk Cho, Ho-Young Lee, Yang-Kyu Choi, Jung-ah Choi, Manki Song, Man-Seong Park, Jun-Young Seo, Jeon-Soo Shin, Jun-Won Yun, Ki Taek Nam, and Je Kyung Seong.

Methodology, Hyuna Noh, Suhyeon Yoon, Sung-Hee Kim, Jiseon Kim, Jung Seon Seo, Jeong Jin Kim, In Ho Park, Jooyeon Oh, Joon-Yong Bae, Gee Eun Lee, Sun-Je Woo, Sun-Min Seo, Na-Won Kim, Youn Woo Lee, Hui Jeong Jang, Seung-Min Hong, Se-Hee An, Kwang-Soo Lyoo, Minjoo Yeom, Hanbyeul Lee, Bud Jung, Sun-Woo Yoon, Jung-Ah Kang, Sang-Hyuk Seok, Yu Jin Lee, Seo Yeon Kim, Young Been Kim, Ji-Yeon Hwang, Dain On, Soo-Yeon Lim, Sol Pin Kim, and Ji Yun Jang.

Funding **acquisition**, Je Kyung Seong.

Resources, Daesub Song, Kang-Seuk Cho, Ho-Young Lee, Yang-Kyu Choi, Jung-ah Choi, Manki Song, Man-Seong Park, Jun-Young Seo, Jeon-Soo Shin, Ki Taek Nam, and Je Kyung Seong.

Supervision, Jun-Won Yun, Ki Taek Nam, and Je Kyung Seong.

Writing - original draft, Jun-Won Yun, Ki Taek Nam, and Je Kyung Seong.

Writing - review & editing, Jun-Won Yun and Je Kyung Seong.

Declaration of competing interest

The authors declare that they have no conflict of interest.

Data availability

Data will be made available on request.

Acknowledgements

This research was supported by a National Research Foundation of Korea (NRF) grant funded by the Korean government (MSIT) (2020M3A9I2109027 and 2021M3H9A1030260).

References

[1] N. Kahn, New virus discovered by Chinese scientists investigating pneumonia outbreak, Wall St. J. 8 (2020).
[2] D.M. Morens, P. Daszak, J.K. Taubenberger, Escaping pandora's box - another novel coronavirus, N. Engl. J. Med. 382 (14) (2020) 1293–1295.
[3] J.M. Sanders, M.L. Monogue, T.Z. Jodlowski, J.B. Cutrell, Pharmacologic treatments for coronavirus disease 2019 (COVID-19): a review, JAMA 323 (18) (2020) 1824–1836.
[4] M. Hoffmann, H. Kleine-Weber, S. Schroeder, N. Kruger, T. Herrler, S. Erichsen, T. S. Schiergens, G. Herrler, N.H. Wu, A. Nitsche, M.A. Muller, C. Drosten, S. Pohlmann, SARS-CoV-2 cell entry Depends on ACE2 and TMPRSS2 and is blocked by a clinically proven protease inhibitor, Cell 181 (2) (2020) 271–+.
[5] R. Wu, L. Wang, H.D. Kuo, A. Shannar, R. Peter, P.J. Chou, S. Li, R. Hudlikar, X. Liu, Z. Liu, G.J. Poiani, L. Amorosa, L. Brunetti, A.N. Kong, An update on current therapeutic drugs treating COVID-19, Curr Pharmacol Rep 6 (3) (2020) 56–70.
[6] M. Levi, J. Thachil, T. Iba, J.H. Levy, Coagulation abnormalities and thrombosis in patients with COVID-19, Lancet Haematol 7 (6) (2020) e438–e440.
[7] S.H. Nile, A. Nile, J. Qiu, L. Li, X. Jia, G. Kai, COVID-19: pathogenesis, cytokine storm and therapeutic potential of interferons, Cytokine Growth Factor Rev. 53 (2020) 66–70.
[8] C. Zhang, C. Zhou, L. Shi, G. Liu, Perspectives on development of vaccines against severe acute respiratory syndrome coronavirus 2 (SARS-CoV-2), Hum. Vaccines Immunother. 16 (10) (2020) 2366–2369.
[9] Y.R. Guo, Q.D. Cao, Z.S. Hong, Y.Y. Tan, S.D. Chen, H.J. Jin, K.S. Tan, D.Y. Wang, Y. Yan, The origin, transmission and clinical therapies on coronavirus disease 2019 (COVID-19) outbreak - an update on the status, Military Med Res 7 (1) (2020) 1–10.
[10] J. Abraham, Passive antibody therapy in COVID-19, Nat. Rev. Immunol. 20 (7) (2020) 401–403.
[11] J. Santos, S. Brierley, M.J. Gandhi, M.A. Cohen, P.C. Moschella, A.B.L. Declan, Repurposing therapeutics for potential treatment of SARS-CoV-2: a review, Viruses 12 (7) (2020) 705.
[12] L.H. Lancaster, J.A. de Andrade, J.D. Zibrak, M.L. Padilla, C. Albera, S.D. Nathan, M.S. Wijsenbeek, J.L. Stauffer, K.U. Kirchgaessler, U. Costabel, Pirfenidone safety and adverse event management in idiopathic pulmonary fibrosis, Eur. Respir. Rev. 26 (146) (2017).
[13] F. Ferrara, G. Granata, C. Pelliccia, R. La Porta, A. Vitiello, The added value of pirfenidone to fight inflammation and fibrotic state induced by SARS-CoV-2 : anti-inflammatory and anti-fibrotic therapy could solve the lung complications of the infection? Eur. J. Clin. Pharmacol. 76 (11) (2020) 1615–1618.
[14] S.J. Cleary, S.C. Pitchford, R.T. Amison, R. Carrington, C.L. Robaina Cabrera, M. Magnen, M.R. Looney, E. Gray, C.P. Page, Animal models of mechanisms of SARS-CoV-2 infection and COVID-19 pathology, Br. J. Pharmacol. 177 (21) (2020) 4851–4865.
[15] M. Imai, K. Iwatsuki-Horimoto, M. Hatta, S. Loeber, P.J. Halfmann, N. Nakajima, T. Watanabe, M. Ujie, K. Takahashi, M. Ito, S. Yamada, S.F. Fan, S. Chiba, M. Kuroda, L.Z. Guan, K. Takada, T. Armbrust, A. Balogh, Y. Furusawa, M. Okuda, H. Ueki, A. Yasuhara, Y. Sakai-Tagawa, T.J.S. Lopes, M. Kiso, S. Yamayoshi, N. Kinoshita, N. Ohmagari, S. Hattori, M. Takeda, H. Mitsuya, F. Krammer, T. Suzuki, Y. Kawaoka, Syrian hamsters as a small animal model for SARS-CoV-2 infection and countermeasure development, P Natl Acad Sci USA 117 (28) (2020) 16587–16595.
[16] L. Bao, W. Deng, B. Huang, H. Gao, J. Liu, L. Ren, Q. Wei, P. Yu, Y. Xu, F. Qi, Y. Qu, F. Li, Q. Lv, W. Wang, J. Xue, S. Gong, M. Liu, G. Wang, S. Wang, Z. Song, L. Zhao, P. Liu, L. Zhao, F. Ye, H. Wang, W. Zhou, N. Zhu, W. Zhen, H. Yu, X. Zhang, L. Guo, L. Chen, C. Wang, Y. Wang, X. Wang, Y. Xiao, Q. Sun, H. Liu, F. Zhu, C. Ma, L. Yan, M. Yang, J. Han, W. Xu, W. Tan, X. Peng, Q. Jin, G. Wu, C. Qin, The pathogenicity of SARS-CoV-2 in hACE2 transgenic mice, Nature 583 (7818) (2020) 830–833.
[17] S. Flint, W. Enquist, V. Racaniello, A. Skalka, Virological Metyhods in Principles of Virology, ASM Press, 2009.

[18] R. Klopfleisch, Multiparametric and semiquantitative scoring systems for the evaluation of mouse model histopathology–a systematic review, BMC Vet. Res. 9 (1) (2013) 123.
[19] C.L. Scudamore, Practical approaches to reviewing and recording pathology data, A Practical Guide to Histology of the Mouse (2014) 25–41.
[20] A.S. Reynolds, A.G. Lee, J. Renz, K. DeSantis, J. Liang, C.A. Powell, C. E. Ventetuolo, H.D. Poor, Pulmonary vascular dilatation detected by automated transcranial Doppler in COVID-19 pneumonia, Am. J. Respir. Crit. Care Med. 202 (7) (2020) 1037–1039.
[21] E.S. Winkler, A.L. Bailey, N.M. Kafai, S. Nair, B.T. McCune, J. Yu, J.M. Fox, R. E. Chen, J.T. Earnest, S.P. Keeler, SARS-CoV-2 infection of human ACE2-transgenic mice causes severe lung inflammation and impaired function, Nat. Immunol. 21 (11) (2020) 1327–1335.
[22] Q. Xiang, Z. Feng, B. Diao, C. Tu, Q. Qiao, H. Yang, Y. Zhang, G. Wang, H. Wang, C. Wang, L. Liu, C. Wang, L. Liu, R. Chen, Y. Wu, Y. Chen, SARS-CoV-2 induces lymphocytopenia by promoting inflammation and Decimates secondary lymphoid organs, Front. Immunol. 12 (2021), 661052.
[23] G.M. Nitulescu, H. Paunescu, S.A. Moschos, D. Petrakis, G. Nitulescu, G.N.D. Ion, D.A. Spandidos, T.K. Nikolouzakis, N. Drakoulis, A. Tsatsakis, Comprehensive analysis of drugs to treat SARS-CoV-2 infection: mechanistic insights into current COVID-19 therapies (Review), Int. J. Mol. Med. 46 (2) (2020) 467–488.
[24] P. Tarighi, S. Eftekhari, M. Chizari, M. Sabernavaei, D. Jafari, P. Mirzabeigi, A review of potential suggested drugs for coronavirus disease (COVID-19) treatment, Eur. J. Pharmacol. 895 (2021), 173890.
[25] J.K. Yella, S. Yaddanapudi, Y. Wang, A.G. Jegga, Changing Trends in Computational Drug Repositioning, Pharmaceuticals (Basel) 11 (2) (2018) 57.
[26] P.B. McCray Jr., L. Pewe, C. Wohlford-Lenane, M. Hickey, L. Manzel, L. Shi, J. Netland, H.P. Jia, C. Halabi, C.D. Sigmund, Lethal infection of K18-hACE2 mice infected with severe acute respiratory syndrome coronavirus, J. Virol. 81 (2) (2007) 813–821.
[27] S. Kumar, P.K. Yadav, R. Srinivasan, N. Perumal, Selection of animal models for COVID-19 research, Virusdisease 31 (4) (2020) 453–458.
[28] F.S. Oladunni, J.G. Park, P.A. Pino, O. Gonzalez, A. Akhter, A. Allue-Guardia, A. Olmo-Fontanez, S. Gautam, A. Garcia-Vilanova, C. Ye, K. Chiem, C. Headley, V. Dwivedi, L.M. Parodi, K.J. Alfson, H.M. Staples, A. Schami, J.I. Garcia, A. Whigham, R.N. Platt 2nd, M. Gazi, J. Martinez, C. Chuba, S. Earley, O. H. Rodriguez, S.D. Mdaki, K.N. Kavelish, R. Escalona, C.R.A. Hallam, C. Christie, J. L. Patterson, T.J.C. Anderson, R. Carrion Jr., E.J. Dick Jr., S. Hall-Ursone, L. S. Schlesinger, X. Alvarez, D. Kaushal, L.D. Giavedoni, J. Turner, L. Martinez-Sobrido, J.B. Torrelles, Lethality of SARS-CoV-2 infection in K18 human angiotensin-converting enzyme 2 transgenic mice, Nat. Commun. 11 (1) (2020) 6122.
[29] R.H. David Smith, in: L.a.s. association (Ed.), The Selection of Non-rodent Species for Pharmaceutical Toxicology, Laboratory animal science association, 2001.
[30] Y.W. Son, H.N. Choi, J.H. Che, B.C. Kang, J.W. Yun, Advances in selecting appropriate non-rodent species for regulatory toxicology research: policy, ethical, and experimental considerations, Regul. Toxicol. Pharmacol. 116 (2020), 104757.
[31] H. Jeong, Y.W. Lee, I.H. Park, H. Noh, S.H. Kim, J. Kim, D. Jeon, H.J. Jang, J. Oh, D. On, C. Uhm, K. Cho, H. Oh, S. Yoon, J.S. Seo, J.J. Kim, S.H. Seok, Y.J. Lee, S. M. Hong, S.H. An, S.Y. Kim, Y.B. Kim, J.Y. Hwang, H.J. Lee, H.B. Kim, D.G. Jeong, D. Song, M. Song, M.S. Park, K.S. Choi, J.W. Park, J.Y. Seo, J.W. Yun, J.S. Shin, H. Y. Lee, K.T. Nam, J.K. Seong, Comparison of the pathogenesis of SARS-CoV-2 infection in K18-hACE2 mouse and Syrian golden hamster models, Dis Model Mech 15 (11) (2022), dmm049632.
[32] J.F. Chan, A.J. Zhang, S. Yuan, V.K. Poon, C.C. Chan, A.C. Lee, W.M. Chan, Z. Fan, H.W. Tsoi, L. Wen, R. Liang, J. Cao, Y. Chen, K. Tang, C. Luo, J.P. Cai, K.H. Kok, H. Chu, K.H. Chan, S. Sridhar, Z. Chen, H. Chen, K.K. To, K.Y. Yuen, Simulation of the clinical and pathological manifestations of coronavirus disease 2019 (COVID-19) in a golden Syrian hamster model: implications for disease pathogenesis and transmissibility, Clin. Infect. Dis. 71 (9) (2020) 2428–2446.
[33] K.M. White, R. Rosales, S. Yildiz, T. Kehrer, L. Miorin, E. Moreno, S. Jangra, M. B. Uccellini, R. Rathnasinghe, L. Coughlan, C. Martinez-Romero, J. Batra, A. Rojc, M. Bouhaddou, J.M. Fabius, K. Obernier, M. Dejosez, M.J. Guillen, A. Losada, P. Aviles, M. Schotsaert, T. Zwaka, M. Vignuzzi, K.M. Shokat, N.J. Krogan, A. Garcia-Sastre, Plitidepsin has potent preclinical efficacy against SARS-CoV-2 by targeting the host protein eEF1A, Science 371 (6532) (2021) 926–+.
[34] C.D. Spinner, R.L. Gottlieb, G.J. Criner, J.R.A. Lopez, A.M. Cattelan, A. S. Viladomiu, O. Ogbuagu, P. Malhotra, K.M. Mullane, A. Castagna, L.Y.A. Chai, M. Roestenberg, O.T.Y. Tsang, E. Bernasconi, P. Le Turnier, S.C. Chang, D. SenGupta, R.H. Hyland, A.O. Osinusi, H.Y. Cao, C. Blair, H.Y. Wang, A. Gaggar, D.M. Brainard, M.J. McPhail, S. Bhagani, Y. Ahn, A.J. Sanyal, G. Huhn, F.M. Marty, G.-U.-.- Investigators, Effect of remdesivir vs standard Care on clinical status at 11 Days in patients with moderate COVID-19 A randomized clinical trial, JAMA, J. Am. Med. Assoc. 324 (11) (2020) 1048–1057.
[35] Y. Wang, D. Zhang, G. Du, R. Du, J. Zhao, Y. Jin, S. Fu, L. Gao, Z. Cheng, Q. Lu, Y. Hu, G. Luo, K. Wang, Y. Lu, H. Li, S. Wang, S. Ruan, C. Yang, C. Mei, Y. Wang, D. Ding, F. Wu, X. Tang, X. Ye, Y. Ye, B. Liu, J. Yang, W. Yin, A. Wang, G. Fan, F. Zhou, Z. Liu, X. Gu, J. Xu, L. Shang, Y. Zhang, L. Cao, T. Guo, Y. Wan, H. Qin, Y. Jiang, T. Jaki, F.G. Hayden, P.W. Horby, B. Cao, C. Wang, Remdesivir in adults with severe COVID-19: a randomised, double-blind, placebo-controlled, multicentre trial, Lancet 395 (10236) (2020) 1569–1578.
[36] R.C. Group, Dexamethasone in hospitalized patients with Covid-19, N. Engl. J. Med. 384 (8) (2021) 693–704.
[37] W.S.T. Consortium, Repurposed antiviral drugs for Covid-19—interim WHO solidarity trial results, N. Engl. J. Med. 384 (6) (2021) 497–511.
[38] S.F. Sia, L.M. Yan, A.W.H. Chin, K. Fung, K.T. Choy, A.Y.L. Wong, P. Kaewpreedee, R. Perera, L.L.M. Poon, J.M. Nicholls, M. Peiris, H.L. Yen, Pathogenesis and transmission of SARS-CoV-2 in golden hamsters, Nature 583 (7818) (2020) 834–838.
[39] S.H. Hodgson, K. Mansatta, G. Mallett, V. Harris, K.R.W. Emary, A.J. Pollard, What defines an efficacious COVID-19 vaccine? A review of the challenges assessing the clinical efficacy of vaccines against SARS-CoV-2, Lancet Infect. Dis. 21 (2) (2021) E26–E35.
[40] H.F. Florindo, R. Kleiner, D. Vaskovich-Koubi, R.C. Acurcio, B. Carreira, E. Yeini, G. Tiram, Y. Liubomirski, R. Satchi-Fainaro, Immune-mediated approaches against COVID-19, Nat. Nanotechnol. 15 (8) (2020) 630–645.
[41] M. Nord, T.N. Cassel, H. Braun, G. Suske, Regulation of the Clara cell secretory protein/uteroglobin promoter in lung, Ann. N. Y. Acad. Sci. 923 (1) (2000) 154–165.
[42] F. Broeckaert, A. Bernard, Clara cell secretory protein (CC16): characteristics and perspectives as lung peripheral biomarker, Clin. Exp. Allergy 30 (4) (2000) 469–475.
[43] T. Weaver, J. Conkright, Function of Surfactant Proteins B and C, Annu Rev Physiol, 2001.